Isotopic signatures and source apportionment of Pb in ambient PM2.5

Chien-Cheng Jung
China Medical University
Charles Chou (ckchou@rcec.sinica.edu.tw)
Academia Sinica
Yi-Tang Huang
Academia Sinica
Shih-Yu Chang
Chung Shan Medical University
Chung-Te Lee
National Central University
Chuan-Yao Lin
Academia Sinica
Hing-Cho Cheung
Sun Yat-sen University
Weu-Chen Kuo
Meteorological Research Institute
Chih-Wei Chang
Environmental Protection Administration
Shuenn-Chin Chang
Environmental Protection Administration

Research Article

Keywords: particulate, source, isotopic, composition, contribution

Posted Date: October 19th, 2021

DOI: https://doi.org/10.21203/rs.3.rs-959808/v1

Version of Record: A version of this preprint was published at Scientific Reports on March 14th, 2022. See the published version at https://doi.org/10.1038/s41598-022-08096-1.

Isotopic signatures and source apportionment of Pb in ambient $PM_{2.5}$

Chien-Cheng Jung[1], Charles C.-K. Chou[2*], Yi-Tang Huang[2], Shih-Yu Chang[3], Chung-Te Lee[4], Chuan-Yao Lin[2], Hing-Cho Cheung[5,6], Wei-Chen Kuo[7], Chih-Wei Chang[8], Shuenn-Chin Chang[8, 9]

[1]Department of Public Health, China Medical University, Taichung, Taiwan

[2]Research Center for Environmental Changes, Academia Sinica, Taipei, Taiwan

[3]Department of Public Health, Chung Shan Medical University, Taichung, Taiwan

[4]Graduate Institute of Environmental Engineering, National Central University, Taoyuan, Taiwan

[5]School of Atmospheric Sciences and Guangdong Province Key Laboratory for Climate Change and Natural Disaster Studies, Sun Yat-Sen University, Guangzhou, China

[6]Southern Marine Science and Engineering Guangdong Laboratory, Zhuhai, China

[7]Meteorological Research Institute (MRI), Tsukuba, Japan

[8]Environmental Protection Administration, Taipei, Taiwan

[9]School of Public Health, National Defense Medical Center, Taipei, Taiwan

*Corresponding author:

Charles C.-K. Chou (ckchou@rcec.sinica.edu.tw)

Research Fellow

Research Center for Environmental Changes, Academia Sinica

Abstract

Particulate lead (Pb) is a primary air pollutant that affects society because of its health impacts. This study investigates the source sectors of Pb associated with ambient fine particulate matter ($PM_{2.5}$) over central-western Taiwan (CWT) with new constraints on the Pb-isotopic composition. We demonstrate that the contribution of coal-fired facilities is overwhelming, which is estimated to reach 35±16 % in the summertime and is enhanced to 57±24 % during the winter monsoon seasons. Moreover, fossil-fuel vehicles remain a major source of atmospheric Pb, which accounts for 12±5 %, despite the current absence of a leaded gasoline supply. Significant seasonal and geographical variations in the Pb-isotopic composition are revealed, which suggest that the impact of East Asian (EA) pollution outflows is important in north CWT and drastically declines toward the south. We estimate the average contribution of EA outflows as accounting for 35±15 % (3.6±1.5 ng/m^3) of the atmospheric Pb loading in CWT during the winter monsoon seasons.

Introduction

Scientific studies have demonstrated that exposure to lead (Pb) particles is associated with hypertension [1, 2]. It has also been indicated that a Pb level higher than 10 mg/dL in blood could result in a decline in the birth weight of infants [3] and intellectual impairment in children [4]. Studies have found that even low-level Pb exposure could cause damage to the nervous system [5, 6] and hippocampus [7, 8] and increase the risk of cognitive dysfunction [9].

In the 1970s, Pb-alkyl additives in gasoline were a major source of Pb in the atmosphere [10, 11]. Given the scientific evidence of the health impacts of lead exposure, the use of leaded fuels had been banned by some national governments in the 1980s and a worldwide phase-out was just announced by the United Nations Environment Programme (UNEP) recently. Consequently, a notable reduction in the ambient Pb level was achieved. For example, the Pb level sharply declined from 1.5 μg/m^3 in 1975 to 0.07 μg/m^3 in 1990 in the US [12] and from 700 ng/m^3 in 1991 to 2.6 ng/m^3 in 2015 in Taipei, Taiwan [13, 14, 15]. However, elevated Pb levels have still been observed in recent studies, suggesting substantial air quality impacts of other sources [13, 14, 16, 17, 18, 19]. Therefore, Pb remains a critical public health concern [20]. Investigations on the sources of Pb-containing particles have therefore been conducted, which have reported emissions of Pb stemming from a wide range of sources including but not limited to road dust, incinerators, coal-fired power plants, mines, bedrock, and construction work [21, 22, 23, 24, 25, 26, 27].

Because Pb-containing particles originating from various sources usually occur mixed in ambient fine particulate matter ($PM_{2.5}$), the identification and apportionment of sources of Pb particles is a highly challenging issue in air quality management. The positive matrix factorization (PMF) model is a statistical tool that is widely applied in air pollution investigations [13, 27, 28, 29] and can resolve the contribution matrix of particulate matter pollution sources according to profiles of the chemical composition. However, the attribution of each factor to a specific pollution source is highly uncertain because the chemical profiles of pollution sources may exhibit common features [30]. Recently, scientists have explored the

isotopic characteristics of Pb collected from specific sources or ambient air [31, 32, 33, 34] and, in turn, have assessed the impacts of various sources [14, 25, 35, 36]. Studies have determined that the Pb isotopic composition changes due to variations in oil consumption and unleaded gasoline usage [37, 38, 39] and have suggested the major role of industrial emissions in present-day Pb pollution.

Taiwan is located offshore of southeastern China and is thus subject to the impacts of air pollution associated with East Asian (EA) continental outflows during the winter monsoon seasons. In addition, western Taiwan is a highly developed area with a population of approximately 23 million people and a large number of industrial factories, which emit a substantial amount of air pollutants. In this study, we include the isotopic composition of Pb in the chemical profile of $PM_{2.5}$ samples collected in central-western Taiwan (CWT) from 2016–2018. The Pb isotopic features of each pollution factor are then resolved with the PMF model, which adds new dimensions in source apportionment and helps to attribute Pb pollution to specific sources. Moreover, analysis of the geographical distribution of the Pb isotope ratios (i.e., $^{206}Pb/^{207}Pb$ and $^{208}Pb/^{207}Pb$) of $PM_{2.5}$ samples is conducted to investigate the influences of air pollution originating from local sources and/or transported by EA continental outflows during the winter monsoon seasons.

Results

Ambient concentration and mass mixing ratio of Pb in $PM_{2.5}$

Analysis of the samples collected under the $PM_{2.5}$ speciation program of the Taiwan Environmental Protection Administration (EPA) revealed that, during the period from 2017–2019, the average ambient concentration of Pb in $PM_{2.5}$ reached 7.9±8.2, 8.3±7.4 and 16.0±22.1 ng/m^3 at the Zhongming (ZM), Douliu (DL), and Chiayi (CY) stations, respectively. The geographical locations of these sampling sites are shown in Supplementary Fig. 1. The results indicate that the Pb concentrations at ZM and DL are highly correlated (r = 0.7386), whereas

90 the Pb concentration at CY exhibits significantly different features ($p < 0.01$). In contrast, the
91 corresponding $PM_{2.5}$ levels were 21.1±11.5, 26.3±14.3, and 26.5±15.0 μg/m^3 at the three
92 stations from 2017–2019. The $PM_{2.5}$ collected at CY is characterized by an average Pb mass
93 mixing ratio of 533±613 ppm, which is 51 % and 85 % higher than the ratios of 354±271 ppm
94 and 289±178 ppm, reported at the ZM and DL stations, respectively.

95 Figure 1 shows that both the ambient concentration and mass mixing ratio of Pb in $PM_{2.5}$
96 are associated with significant seasonal variations. The decline in the ambient Pb concentration
97 in summer agrees with the typical air pollution pattern, which is usually the result of
98 atmospheric dispersion enhancement. However, the amplitude of the seasonal variation in the
99 Pb concentration (i.e., winter mean/summer mean) ranges from 3.8–10.2 at the three sites,
100 which is significantly larger than the amplitude of the variation in $PM_{2.5}$. The seasonal variation
101 in the mass mixing ratio of Pb in $PM_{2.5}$ suggests that Pb more abundantly occurs in $PM_{2.5}$ during
102 the period from September to April of the next year, which indicates that the sources of $PM_{2.5}$
103 change with the seasons in CWT. Considering the geographic location of Taiwan and the
104 transport of air masses by monsoons from East Asia, the study area is subject to continental
105 pollution outbreaks during the EA winter monsoon seasons. The transport of Pb-containing
106 particles with continental outflows to northern Taiwan has been reported in an earlier study [14].
107 In addition, the seasonal variations shown in Fig. 1 are consistent with the seasonality of EA
108 continental outflows [40]. However, the transport of air pollutants from upwind Taiwanese coastal
109 zones, where emission sources of Pb-containing particles such as ships and harbor facilities,
110 coal-fired power plants, and other industrial factories are located, are also suspected.

111 **Isotopic composition of Pb in $PM_{2.5}$**

112 Table 1 summarizes the isotopic composition of Pb in the $PM_{2.5}$ samples collected during
113 the intensive investigation from 2016–2018 in this study. The overall average $PM_{2.5}$
114 concentration was 23.5±13.7 μg/m^3 in the study area, ranging from 20.0±13.0 to 25.9±17.0
115 μg/m^3 at the respective sites. The overall average ambient Pb concentration in $PM_{2.5}$ was

8.6±7.2 ng/m^3, with the site-specific average concentrations ranging from 3.3±2.2 to 15.6±12.7 ng/m^3. While the overall average ambient Pb level during the sampling campaigns is comparable to that reported in the previous section, this investigation reveals pronounced spatial differences in the ambient Pb concentration.

The overall average values of the $^{206}Pb/^{207}Pb$ and $^{208}Pb/^{207}Pb$ ratios were 1.148±0.009 and 2.427±0.012, respectively. Considering the potential seasonal changes in the sources of Pb in $PM_{2.5}$, the sampling campaigns were further divided into summer (i.e., August 2017 and July 2018) and winter (November 2016, February 2017 and March 2018) campaigns. The summer average values of $^{206}Pb/^{207}Pb$ and $^{208}Pb/^{207}Pb$ were 1.145±0.010 and 2.419±0.011, respectively, whereas the winter average values reached 1.150±0.008 and 2.432±0.011, respectively. Both isotopic ratios exhibited significant seasonal differences ($p < 0.01$). Figure 2 illustrates the correlation between $^{206}Pb/^{207}Pb$ and $^{208}Pb/^{207}Pb$. In general, these two isotopic ratios maintained a significant linear correlation, whereas a steeper slope was associated with the winter dataset. A larger slope value generally indicates a significant increase in the relative abundance of ^{208}Pb during the winter monsoon seasons. Moreover, it should be noted that both $^{206}Pb/^{207}Pb$ and $^{208}Pb/^{207}Pb$ exhibited an increasing trend and moved toward the case representing EA continental outflows (as shown in Fig. 2) during the winter monsoon seasons.

Source identification of Pb in $PM_{2.5}$

To resolve the contribution of the pollution sources responsible for Pb in $PM_{2.5}$, this study employed the PMF model to analyze the data obtained during the intensive investigation. Note that the 3 Pb isotopes (^{206}Pb, ^{207}Pb, and ^{208}Pb) were independently considered in the chemical profiles, and the retrieved factors were in turn characterized based on Pb isotopic ratios (i.e., $^{206}Pb/^{207}Pb$ and $^{208}Pb/^{207}Pb$). PMF analysis provided a solution involving 8 factors. However, considering the uncertainties associated with the measurements and source apportionment, we examined only the top 4 factors, which accounted for ~80 % of the total Pb in $PM_{2.5}$, in this study. Attribution of the source factors was based on the characteristic elements of the chemical

profiles. In summary, the four major source factors of Pb included the following: 1.) traffic emissions, 2.) the petrol industry, 3.) coal-fired facilities, and 4.) oil-fired facilities. Notably, all four major sources were related to the production and/or use of fossil fuels. The chemical profiles of the respective factors are shown in Supplementary Fig. 2. Table 2 summarizes the contribution of each source factor to the total Pb in $PM_{2.5}$ in the study area and the Pb isotopic ratios and characteristic elements considered to achieve source attribution. Note that the above attribution of source factors resolved by the PMF model was based simply on the characteristic elements illustrated in the chemical profiles, but there could be contributions of unidentified minor sources not accounted for.

The contribution of traffic emissions (Factor 1) to Pb in $PM_{2.5}$ was estimated to reach 12±5 % in the study area despite the current lack of leaded gasoline usage. The attribution of this factor was based not only on the dominance of the variations in Cu, Mn and Zn in $PM_{2.5}$ but also on the Pb isotopic ratios. This factor was characterized by $^{206}Pb/^{207}Pb$ and $^{208}Pb/^{207}Pb$ ratios of 1.146 and 2.418, respectively. As shown in Fig. 2, the Pb isotopic features are consistent with the features of gasoline and diesel supplied in Taiwan [41].

The second source factor was attributed to the petrol industry due to the abundance of source-specific characteristic elements, in particular La, Ce, and Nd [42]. The contribution of this factor was estimated to reach 11±4 % throughout the entire study period, whereas a higher contribution (16±8 %) was observed in summer. This is justified by the geographic location of local sources in the study area. Several petroleum refining factories are located in southern Taiwan, which occurs upwind of our study sites during the summer monsoon seasons.

Coal-fired facilities (Factor 3) contributed almost half (49±12 %) of Pb in $PM_{2.5}$ in this area. This source factor exhibited significant seasonal differences, contributing 35±16 % to the Pb loading during the summer campaigns and 57±24 % during the winter campaigns on average. This factor was characterized by $^{206}Pb/^{207}Pb$ and $^{208}Pb/^{207}Pb$ ratios of 1.159 and 2.467, respectively. As shown in Fig. 2, this Pb isotopic feature is similar to that of aerosol samples

168 collected in Chinese urban areas with significant pollution attributed to coal combustion [39]. It
169 has been previously reported that the concentration and mixing ratio of Pb in $PM_{2.5}$ are
170 enhanced during the EA winter monsoon seasons, suggesting influences of pollution
171 transported from eastern and/or northern China. Here, the argument is further supported by Pb
172 isotope evidence.

173 The 4th source factor encompassed oil-fired facilities because the variations in Ni and V
174 in $PM_{2.5}$ were predominant. Given that residue oil is used mostly in heavy duty engines and
175 boilers, this source was likely related to the emissions of ships and industrial facilities. This
176 factor contributed 10±5 % to the Pb loading throughout the entire study period, whereas a
177 significantly high contribution (21±8 %) was estimated during the summer campaigns. This
178 seasonality was further justified by the geographic distribution of pollution sources in Taiwan.
179 The majority of the heavy industry is located in southern Taiwan. Moreover, this factor could
180 have been influenced by local circulation because sea breezes prevail in summer and thus could
181 transport more ship emissions from the Taiwan Strait into the study area.

182

183 **Discussion**

184 **Pb isotopic fingerprints of coal-fired facilities**

185 The results in this study indicate that the ambient concentration and mass mixing ratio of
186 Pb in $PM_{2.5}$ over CWT were significantly higher during the EA winter monsoon seasons than
187 those during the summertime. Analysis of the back-trajectories of the air masses arriving in the
188 study area on the sampling days reveals that Taiwan was influenced by EA outflows during the
189 winter campaign periods and by southwesterlies during the summer campaign periods (as
190 shown in Supplementary Fig. 3). PMF analysis determined the predominant factor of the
191 contribution of coal-fired facilities (F3), which accounted for 57±24 % of the ambient Pb
192 loading during the wintertime. Accordingly, it is plausible that the emission of Pb-containing
193 particles by coal-fired facilities in China is a predominant source of atmospheric Pb in the CWT

194 area during the wintertime. However, PMF analysis also determined a substantial contribution
195 (35±16 %) of this factor (F3) during the summer campaigns, when Taiwan is typically impacted
196 by southwesterly monsoons and isolated from the influences of Chinese air pollution. Thus,
197 there could occur local coal-fired facilities possessing certain Pb isotope fingerprints, such as
198 that of F3 ($^{206}Pb/^{207}Pb$: 1.159±0.004, $^{208}Pb/^{207}Pb$: 2.467±0.006). Within this context, an
199 investigation of the Pb isotopic features of the coal used by local suspected facilities is
200 warranted to identify the sources of atmospheric Pb in Taiwan.

201 **Geographical distribution of the isotopic composition of Pb in $PM_{2.5}$**

202 This study reveals significant spatial differences in the ambient Pb level among the
203 sampling sites. Based on the previous section, the $PM_{2.5}$ samples collected at the Chiayi (CY)
204 site are more enriched in Pb than those collected at the other sites. The results of our intensive
205 investigation (as listed in Table 1) confirm the high Pb level at CY and indicate lower Pb levels
206 at the Fengyuan (FY) and Shalu (SL) sites. Figure 3 shows the changes in the average ambient
207 Pb level and isotopic ratios at each sampling site with the latitude. It is apparent that the ambient
208 Pb level increases from the northern to the southern parts of the study area, where FY and CY
209 are located at the northern and southern ends, respectively. The average Pb isotopic ratios
210 ($^{206}Pb/^{207}Pb$ and $^{208}Pb/^{207}Pb$) of $PM_{2.5}$ at CY are 1.142±0.006 and 2.421±0.006, respectively,
211 and 1.153±0.007 and 2.421±0.009, respectively, during the winter and summer campaigns,
212 respectively. In contrast to the general seasonal shift in the Pb isotopic ratios presented above
213 and shown in Fig. 3(b), the $^{208}Pb/^{207}Pb$ ratio at CY does not significantly vary with the season.
214 Given the high $^{208}Pb/^{207}Pb$ values associated with Chinese air pollutants, as shown in Fig. 2,
215 the isotopic data suggest that the influences of EA outflows on the Pb level at CY are relatively
216 minor. In contrast, the average Pb isotopic ratios ($^{206}Pb/^{207}Pb$ and $^{208}Pb/^{207}Pb$) of $PM_{2.5}$ at FY
217 during the winter campaigns are 1.160±0.003 and 2.439±0.005, respectively, which are
218 comparable to the characteristics of the aerosols transported by EA outflows, as shown in Fig.
219 2. As a result, it is inferred that FY is significantly influenced by EA outflows during the EA

winter monsoon seasons. Notably, the summer-campaign average values of the $^{206}Pb/^{207}Pb$ and $^{208}Pb/^{207}Pb$ ratios of $PM_{2.5}$ at FY shift to 1.143±0.008 and 2.419±0.010, respectively, which are consistent with the winter Pb isotopic features of $PM_{2.5}$ at CY. These seasonal and geographical shifts in the Pb isotopic features suggest variations in the transport of air pollutants, which will be further elaborated in the following section.

Estimation of the contribution of EA outflows to local Pb loadings

Given the narrow range of $^{208}Pb/^{207}Pb$ during the summertime and the significant spatial and seasonal shifts, as shown in Fig. 3(b), we employ a two-end-member model to estimate the contribution of EA outflows during the winter campaigns in this study. We assume that the overall average $^{208}Pb/^{207}Pb$ value over the summer campaigns, i.e., 2.419±0.011, represents the features of local pollution, while the average $^{208}Pb/^{207}Pb$ value based on Chinese urban measurements, as reported by Bi et al. [39], namely, 2.453±0.009, represents the end member of EA outflows. Note that only the investigations conducted after 2000 are included here, considering the changes in pollution sources across China. As a result, it is estimated that EA outflows contribute 35±15 % or 3.6±1.5 ng/m^3 to the ambient Pb loading over CWT during the winter monsoon seasons. The site-specific estimates are summarized in Supplementary Table 2. It should be noted that the influences of EA outflows are more pronounced along the western coastline and exhibit a declining trend toward the southern and inland (eastern) areas. There are two exceptional cases, namely, Shalu (SL) and Mailiao (ML), where the $PM_{2.5}$ properties could have been dominated by specific sources located near these sampling sites.

Within the context of monsoon activity and the Pb isotopic features of $PM_{2.5}$ described above, the results in this study demonstrate that the influences of EA outflows could have drastically declined within only ~1 degree in latitude, i.e., from FY to CY. This is explained by the development of local circulation in CWT. Figure 4 illustrates the mean surface (1000 hPa) streamlines around Taiwan calculated for January and July from 2016–2018, which represent the general transport patterns of air parcels in winter and summer, respectively. The streamlines

indicate that the main stream of EA outflow is geographically blocked by the Central Mountain Ranges of Taiwan. As a result, a side flow moving toward southeastern Taiwan develops, particularly during the daytime. Consequently, the impacts of EA outflows diminish, and the pollutants emitted in the coastal areas of Taiwan could have dominated the air quality in the southern part of the study area. In contrast, the regional wind field is dominated by slow southerly flows during the summertime, and strong sea breezes could have driven local air pollutants eastward. The seasonal changes in local circulation suitably elucidate the geographical shift in the isotopic composition of Pb in $PM_{2.5}$.

Methods

Study site and sample collection

An intensive experimental investigation on the attribution of Pb in $PM_{2.5}$ was conducted in CWT from 2016–2018. A total of 274 daily $PM_{2.5}$ samples was collected at 13 sites distributed among urban, rural, and industrial zones across the study area (Supplementary Fig. 1) during 5 sampling campaigns. Detailed information on the sampling campaigns is provided in Supplementary Table 1.

At each sampling site, a BGI PQ200 sampler (Mesa Labs, Inc., Butler, NJ, USA) was employed to collect $PM_{2.5}$ on Teflon filters, which were used for gravimetric measurement and analysis of crustal and metal elements (Na, Mg, Al, K, Ca, Ti, V, Cr, Mn, Fe, Co, Ni, Cu, Zn, Ga, Ge, As, Se, Rb, Sr, Y, Zr, Mo, Cd, Sn, Sb, Cs, Ba, La, Ce, Pr, Nd, Hf, and Tl) and Pb isotopes (^{206}Pb, ^{207}Pb, and ^{208}Pb). In addition, a multichannel Super-SASS sampler (Met One Instruments Inc., Grants Pass, OR, USA) was deployed to collect $PM_{2.5}$ on Teflon and tissue quartz-fiber filters. The Teflon filter samples were reserved for the analysis of soluble ions (Na^+, NH_4^+, K^+, Mg^{2+}, Ca^{2+}, Cl^-, NO_3^-, and SO_4^{2-}), whereas the quartz filter samples were reserved to determine the content of anhydrosugars (levoglucosan, mannosan, and galactosan), organic carbon (OC) and elemental carbon (EC). To eliminate possible contamination, all quartz-fiber

filters were prefired at 900 °C for 4 hours before sampling.

In addition to the intensive investigation described above, this study also analyzed the Pb content in the samples collected under the Taiwan EPA $PM_{2.5}$ speciation program from 2017–2019. The Taiwan EPA sampling network comprises six stations distributed across Taiwan, and three of these six sites (CM, DL, and CY) are located within our study area (as shown in Supplementary Fig. 1). Under this program, each sample was collected over a 24-h period, and sampling was conducted regularly at 6-day intervals throughout the year.

Chemical analysis

The chemical analysis procedures for soluble ions, OC, EC, anhydrosugars, and crustal/metal elements are described in previous publications [43, 44, 45]. In summary, each Teflon filter sample (from the Super-SASS device) was shaken with 10 mL deionized water for 60 min, and the extracts were then filtered. Ion chromatography was conducted to analyze the soluble ions in the extracts. The OC and EC concentrations in the quartz filter samples (from the Super-SASS device) were determined with a DRI-2001A carbonaceous aerosol analyzer, following the IMPROVE-A thermo-optical reflectance (TOR) protocol. In addition, a punch (17 mm in diameter) of each quartz filter sample was extracted in 3 mL deionized water for 60 min, and an ion chromatography instrument equipped with a pulsed amperometric detector (PAD) (ICS-5000, Thermo Scientific) was then applied to analyze the contents of levoglucosan, mannosan, and galactosan in the extracts. The Teflon filter samples (from the PQ200 device) were completely dissolved in a mixture of acids in Teflon beakers, i.e., 4 mL HNO_3 (Merck LTD, 60 % ultrapure) and 2 mL HF (Merck LTD, 48 % ultrapure). An inductively coupled plasma-mass spectrometry (ICP-MS) instrument (NexION 300X, Perkin Elmer) was employed to determine the concentrations of crustal/metal elements in the digestion solutions. A fraction of each digestion solution was further purified with Sr-Spec resin (100–150 μm, Eichrom Technologies) in a cleanroom, which was in turn used to analyze Pb isotopes via ICP-MS [14].

Back-trajectory cluster analysis

Analysis of the 5-d back-trajectories of air masses was conducted twice per day using the Hybrid Single-Particle Lagrangian Integrated Trajectory (HYSPLIT) model of the National Oceanic and Atmospheric Administration (NOAA) on the sampling days. The meteorological data considered in the model included 6-hourly Global Data Assimilation System (GDAS) archived data with a resolution of 0.5 degrees in longitude and latitude. The end point of the trajectories occurred 200 m above ground level at the Dali station (24.02° N, 120.677° E), Taichung, Taiwan. Trajectory cluster analysis was then conducted to group trajectories into four clusters.

Data analysis

We adopted the PMF 5.0 model developed by the US EPA to analyze the contribution of respective pollution sources to Pb in $PM_{2.5}$. The basic principle of the PMF model has been described in previous studies [46, 47]. A paired two-tailed t-test was performed to investigate the differences in the chemical composition of $PM_{2.5}$ between the seasons and sampling sites. SAS 9.4 (SAS Institute Inc., Cary, NC, USA) statistical software was employed to analyze all data. Statistical significance was defined at $p < 0.05$.

Data availability

The data that support the findings of this study are available from the corresponding author upon reasonable request.

Competing interests

The authors declare no competing interests.

Acknowledgments

This study received financial support from the Taiwan Environmental Protection Administration under grants EPA-105-U101-02-A272, EPA-105-U102-03-A284, EPA-107-L101-02-A024 and EPA-107-L102-02-A038, the Ministry of Science and Technology under grants 105-2111-M-001-005-MY3 and 106-3114-M-001-001-A, and the Academia Sinica Grand Challenge Program AS-GC-110-01. The authors gratefully acknowledge the logistical support received at the respective sampling sites during the intensive field campaigns.

Author contributions

C.C.K.C. and S.C.C. conceived the Pb isotope research project. C.T.L. and S.C.C. organized the $PM_{2.5}$ speciation network in Taiwan. C.C.K.C. and C.C.J. led the team in data analysis. Y.T.H., S.Y.C. and C.W.C. organized the sampling program. Y.T.H. led the sample collection and chemical analysis. C.Y.L. conducted the streamline analysis. H.C.C. and W.C.K. contributed to cluster analysis of the back-trajectories. C.C.J. and C.C.K.C. wrote the manuscript with contributions from all coauthors.

References

1. Schwartz J. Lead, blood pressure, and cardiovascular disease in men. *Archives of Environmental Health: An International Journal* **50**, 31-37 (1995).
2. Sharp DS, Becker CE, Smith AH. Chronic low-level lead exposure. *Medical Toxicology and Adverse Drug Experience* **2**, 210-232 (1987).
3. Needleman HL, Rabinowitz M, Leviton A, Linn S, Schoenbaum S. The relationship between prenatal exposure to lead and congenital anomalies. *Jama* **251**, 2956-2959 (1984).
4. Canfield RL, Henderson Jr CR, Cory-Slechta DA, Cox C, Jusko TA, Lanphear BP. Intellectual impairment in children with blood lead concentrations below 10 μg per deciliter. *New England journal of medicine* **348**, 1517-1526 (2003).
5. Finkelstein Y, Markowitz ME, Rosen JF. Low-level lead-induced neurotoxicity in children: an update on central nervous system effects. *Brain Research Reviews* **27**, 168-176 (1998).
6. Mason LH, Harp JP, Han DY. Pb neurotoxicity: neuropsychological effects of lead toxicity. *BioMed research international* **2014**, (2014).
7. Jett DA, Kuhlmann AC, Farmer SJ, Guilarte TR. Age-dependent effects of developmental lead exposure on performance in the Morris water maze. *Pharmacology Biochemistry and Behavior* **57**, 271-279 (1997).
8. Slomianka L, Rungby J, West M, Danscher G, Andersen A. Dose-dependent bimodal effect of low-level lead exposure on the developing hippocampal region of the rat: a volumetric study. *Neurotoxicology* **10**, 177-190 (1989).
9. Farooqui Z*, et al.* Associations of cumulative Pb exposure and longitudinal changes in Mini-Mental Status Exam scores, global cognition and domains of cognition: The VA Normative Aging Study. *Environmental research* **152**, 102-108 (2017).

10. Mielke HW, Zahran S. The urban rise and fall of air lead (Pb) and the latent surge and retreat of societal violence. *Environment international* **43**, 48-55 (2012).

11. Patterson Ct. An alternative perspective-lead pollution in the human environment: origin, extent, and significance. *Lead in the human environment*, 265-349 (1980).

12. Callender E, Metre PCV. Environmental policy analysis, peer reviewed: reservoir sediment cores show US lead declines. *Environmental science & technology* **31**, 424A-428A (1997).

13. Hsu C-Y, Chiang H-C, Lin S-L, Chen M-J, Lin T-Y, Chen Y-C. Elemental characterization and source apportionment of PM 10 and PM 2.5 in the western coastal area of central Taiwan. *Science of the Total Environment* **541**, 1139-1150 (2016).

14. Jung C-C*, et al.* C-Sr-Pb isotopic characteristics of PM2.5 transported on the East-Asian continental outflows. *Atmospheric Research*, (2019).

15. Mao I, Chen M. Airborne lead pollution in metropolitan Taipei (Republic of China). *Water, Air, and Soil Pollution* **91**, 375-382 (1996).

16. Tunno BJ, Dalton R, Cambal L, Holguin F, Lioy P, Clougherty JE. Indoor source apportionment in urban communities near industrial sites. *Atmospheric environment* **139**, 30-36 (2016).

17. Schwarz J*, et al.* PM2.5 chemical composition at a rural background site in Central Europe, including correlation and air mass back trajectory analysis. *Atmospheric Research* **176**, 108-120 (2016)

18. Samek L*, et al.* Seasonal variations of chemical composition of PM2.5 fraction in the urban area of Krakow, Poland: PMF source attribution. *Air Quality, Atmosphere & Health* **13**, 89-96 (2020).

19. Nayebare SR*, et al.* Chemical characterization and source apportionment of PM2.5 in Rabigh, Saudi Arabia. *Aerosol and Air Quality Research* **16**, 3114-3129 (2016).

20. O'Connor D*, et al.* Lead-based paint remains a major public health concern: a critical review of global production, trade, use, exposure, health risk, and implications. *Environment international* **121**, 85-101 (2018).

21. Birmili W, Allen AG, Bary F, Harrison RM. Trace metal concentrations and water solubility in size-fractionated atmospheric particles and influence of road traffic. *Environmental Science & Technology* **40**, 1144-1153 (2006).

22. Christian TJ, Yokelson R, Cárdenas B, Molina L, Engling G, Hsu S-C. Trace gas and particle emissions from domestic and industrial biofuel use and garbage burning in central Mexico. *Atmospheric Chemistry and Physics* **10**, 565-584 (2010).

23. Hu C-W*, et al.* Characterization of multiple airborne particulate metals in the surroundings of a municipal waste incinerator in Taiwan. *Atmospheric Environment* **37**, 2845-2852 (2003).

24. Lin Y-C*, et al.* Characteristics of trace metals in traffic-derived particles in Hsuehshan Tunnel, Taiwan: size distribution, potential source, and fingerprinting metal ratio. *Atmospheric Chemistry and Physics* **15**, 4117-4130 (2015).

25. Salcedo D*, et al.* Using trace element content and lead isotopic composition to assess sources of PM in Tijuana, Mexico. *Atmospheric Environment* **132**, 171-178 (2016).

26. Wang C-F, Chang C-Y, Tsai S-F, Chiang H-L. Characteristics of road dust from different sampling sites in northern Taiwan. *Journal of the Air & Waste Management Association* **55**, 1236-1244 (2005).

27. Wang S, Hu G, Yan Y, Wang S, Yu R, Cui J. Source apportionment of metal elements in PM2.5 in a coastal city in Southeast China: Combined Pb-Sr-Nd isotopes with PMF method. *Atmospheric Environment* **198**, 302-312 (2019).

28. Song Y*, et al.* Source apportionment of PM2.5 in Beijing by positive matrix factorization. *Atmospheric Environment* **40**, 1526-1537 (2006).

29. Ho W-Y, Tseng K-H, Liou M-L, Chan C-C, Wang C-H. Application of positive matrix factorization in the identification of the sources of PM2.5 in Taipei City. *International journal of environmental research and public health* **15**, 1305 (2018).

30. Samek L, Stegowski Z, Furman L. Preliminary PM2.5 and PM10 fractions source apportionment complemented by statistical accuracy determination. *Nukleonika* **61**, 75--83 (2016).

31. Widory D, Liu X, Dong S. Isotopes as tracers of sources of lead and strontium in aerosols (TSP & PM 2.5) in Beijing. *Atmospheric environment* **44**, 3679-3687 (2010).

32. Widory D, Roy S, Le Moullec Y, Goupil G, Cocherie A, Guerrot C. The origin of atmospheric particles in Paris: a view through carbon and lead isotopes. *Atmospheric Environment* **38**, 953-961 (2004).

33. Souto-Oliveira C, Babinski M, Araújo D, Weiss D, Ruiz I. Multi-isotope approach of Pb, Cu and Zn in urban aerosols and anthropogenic sources improves tracing of the atmospheric pollutant sources in megacities. *Atmospheric Environment* **198**, 427-437 (2019).

34. Dong S*, et al.* Isotopic signatures suggest important contributions from recycled gasoline, road dust and non-exhaust traffic sources for copper, zinc and lead in PM10 in London, United Kingdom. *Atmospheric Environment* **165**, 88-98 (2017).

35. Hsu S-C, *et al.* Lead isotope ratios in ambient aerosols from Taipei, Taiwan: Identifying long-range transport of airborne Pb from the Yangtze Delta. *Atmospheric Environment* **40**, 5393-5404 (2006).

36. Graney JR, Edgerton ES, Landis MS. Using Pb isotope ratios of particulate matter and epiphytic lichens from the Athabasca Oil Sands Region in Alberta, Canada to quantify local, regional, and global Pb source contributions. *Science of the Total Environment* **654**, 1293-1304 (2019).

37. Komárek M, Ettler V, Chrastný V, Mihaljevič M. Lead isotopes in environmental sciences: a review. *Environment International* **34**, 562-577 (2008).

38. Monna F, Lancelot J, Croudace IW, Cundy AB, Lewis JT. Pb isotopic composition of airborne particulate material from France and the southern United Kingdom: implications for Pb pollution sources in urban areas. *Environmental Science & Technology* **31**, 2277-2286 (1997).

39. Bi X-Y, *et al.* Lead isotopic compositions of selected coals, Pb/Zn ores and fuels in China and the application for source tracing. *Environmental science & technology* **51**, 13502-13508 (2017).

40. Chou CCK, *et al.* Seasonality of the mass concentration and chemical composition of aerosols around an urbanized basin in East Asia. *Journal of Geophysical Research: Atmospheres* **122**, 2026-2042 (2017).

41. Yao P-H, *et al.* Lead isotope characterization of petroleum fuels in Taipei, Taiwan. *International journal of environmental research and public health* **12**, 4602-4616 (2015).

42. Moreno T, *et al.* Lanthanoid geochemistry of urban atmospheric particulate matter. *Environmental Science & Technology* **42**, 6502–6507 (2008).

43. Chang S-Y, Fang G-C, Chou CCK, Chen W-N. Source identifications of PM10

aerosols depending on hourly measurements of soluble components characterization among different events in Taipei Basin during spring season of 2004. *Chemosphere* **65**, 792-801 (2006).

44. Chou CCK*, et al.* Seasonal variation and spatial distribution of carbonaceous aerosols in Taiwan. *Atmospheric Chemistry and Physics* **10**, 9563-9578 (2010).

45. Lin Y-C*, et al.* Wintertime haze deterioration in Beijing by industrial pollution deduced from trace metal fingerprints and enhanced health risk by heavy metals. *Environmental pollution* **208**, 284-293 (2016).

46. Paatero P, Tapper U. Positive matrix factorization: A non-negative factor model with optimal utilization of error estimates of data values. *Environmetrics* **5**, 111-126 (1994).

47. U.S.EPA. EPA Positive Matrix Factorization (PMF) 5.0 Fundamentals and User Guide.). U.S. Environmental Protection Agency (2014).

48. Chow JC*, et al.* Source profiles for industrial, mobile, and area sources in the Big Bend Regional Aerosol Visibility and Observational study. *Chemosphere* **54**, 185-208 (2004).

49. Kulkarni P, Chellam S, Fraser MP. Tracking petroleum refinery emission events using lanthanum and lanthanides as elemental markers for PM2.5. *Environmental science & technology* **41**, 6748-6754 (2007).

50. Okuda T*, et al.* Trends in hazardous trace metal concentrations in aerosols collected in Beijing, China from 2001 to 2006. *Chemosphere* **72**, 917-924 (2008).

51. Querol X*, et al.* Source origin of trace elements in PM from regional background, urban and industrial sites of Spain. *Atmospheric Environment* **41**, 7219-7231 (2007).

52. Cheng M-T, Chio C-P, Huang C-Y, Chen J-M, Wang C-F, Kuo C-Y. Chemical

compositions of fine particulates emitted from oil-fired boilers. *Journal of Environmental Engineering and Management* **18**, 355-362 (2008).

Table 1: Summary of the average concentrations of $PM_{2.5}$ and Pb associated with Pb-isotopic composition during the intensive field investigation

Sampling site	$PM_{2.5}$ ($\mu g/m^3$)	Pb (ng/m^3)	$^{206}Pb/^{207}Pb$	$^{208}Pb/^{207}Pb$
Changhua (CH)	22.6 ± 12.1	9.6 ± 7.1	1.149 ± 0.008	2.429 ± 0.012
Douliu (DL)	24.8 ± 15.4	9.3 ± 7.0	1.145 ± 0.011	2.426 ± 0.015
Dali (DA)	25.0 ± 11.8	5.0 ± 3.9	1.147 ± 0.008	2.426 ± 0.015
Fengyuan (FY)	23.1 ± 9.6	3.7 ± 1.6	1.151 ± 0.010	2.429 ± 0.013
Chiayi (CY)	25.9 ± 17.0	15.6 ± 12.7	1.146 ± 0.008	2.421 ± 0.007
Erlin (EL)	23.7 ± 14.5	10.1 ± 6.5	1.153 ± 0.008	2.430 ± 0.011
Shalu (SL)	24.4 ± 12.5	3.3 ± 2.2	1.137 ± 0.011	2.417 ± 0.013
Xianxi (XX)	24.2 ± 11.7	6.1 ± 4.1	1.152 ± 0.008	2.424 ± 0.010
Xingang (XG)	24.7 ± 15.9	10.1 ± 6.3	1.147 ± 0.008	2.429 ± 0.008
Zhushan (ZS)	22.2 ± 13.5	7.1 ± 5.9	1.146 ± 0.008	2.429 ± 0.010
Mailiao (ML)	21.8 ± 14.1	8.0 ± 5.7	1.149 ± 0.010	2.424 ± 0.013
Lunbei (LB)	25.0 ± 15.7	9.9 ± 6.1	1.149 ± 0.008	2.428 ± 0.013
Taixi (TX)	20.0 ± 13.0	6.9 ± 5.1	1.153 ± 0.010	2.432 ± 0.016
Overall	23.5 ± 13.7	8.6 ± 7.2	1.148 ± 0.009	2.427 ± 0.012

Table 2: Summary of source apportionment for Pb in $PM_{2.5}$ and Pb isotopic composition of the respective source factors resolved by the PMF model

PMF factor (attribution)	Contribution*	$^{206}Pb/^{207}Pb$	$^{208}Pb/^{207}Pb$	Characteristic constituents#
F1 (traffic emissions)	12 ± 5 % (S: 12 ± 6 % W: 12 ± 7 %)	1.146 ± 0.005	2.418 ± 0.009	Zn (51%), Cu (31%), Mn (23%), Pb (12%) (Lin et al. [24])
F2 (petrol industry)	11 ± 4 % (S: 16 ± 8 % W: 8 ± 3 %)	1.148 ± 0.009	2.292 ± 0.008	Nd (56%), Ce (51%), Ti (48%), La (39%), Sr (26%) (Chow [48]; Kulkarni et al.[49]; Moreno et al.[42])
F3 (coal-fired facilities)	49 ± 12 % (S: 35 ± 16 % W: 57 ± 24 %)	1.159 ± 0.004	2.467 ± 0.006	Cd (57%), Pb (52%), As (40%), Se (32%) (Okuda et al. [50])
F4 (oil-fired facilities)	10 ± 5 % (S: 21 ± 8 % W: 6 ± 2 %)	1.126 ± 0.004	2.278 ± 0.005	V (65%), Ni (43%) (Querol et al. [51]; Cheng et al. [52])

* Averages for summer (S) and winter (W) campaigns are listed in parentheses.

The percentage of variations in the characteristic elements attributed to each PMF factor is listed in parentheses.

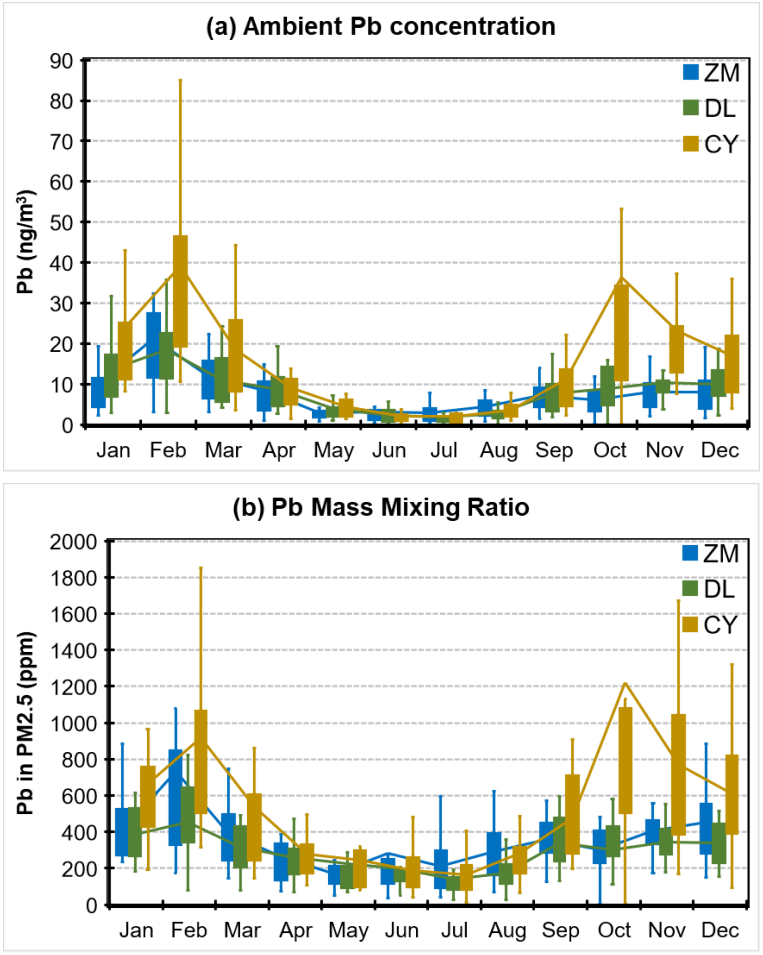

Figure 1: Seasonal variations in the ambient concentrations (a) and mass mixing ratios (b) of Pb in $PM_{2.5}$. Samples are collected at the Zhongming (ZM), Douliu (DL), and Chiayi (CY) sites of the Taiwan EPA $PM_{2.5}$ speciation network from 2017–2019. Geographic information on the sampling sites is shown in Supplementary Fig. 1.

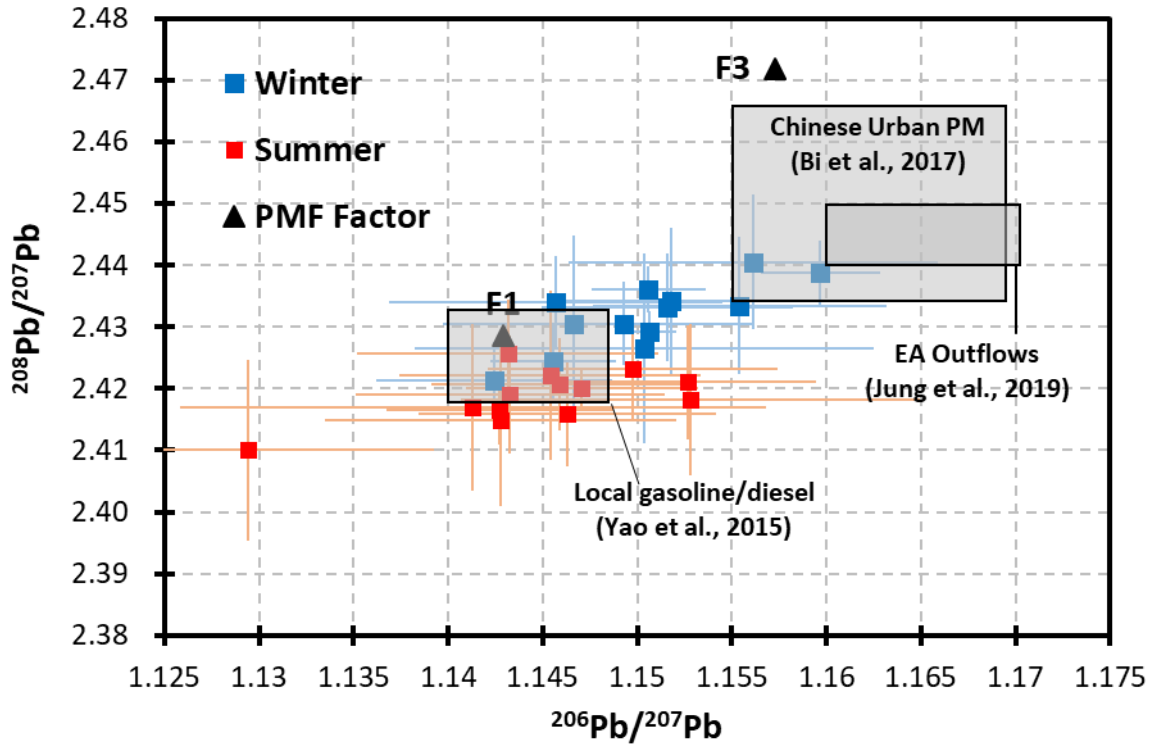

Figure 2: Distribution of the isotopic ratios of Pb in $PM_{2.5}$ in the summer and winter samples. Samples are collected at 13 sampling sites in central-western Taiwan during 5 field campaigns from 2016–2018, as described in the main text. The site-specific averages are denoted by symbols with ranges of +/-1 standard deviation, as shown by the error bars. The isotopic ratios of 2 PMF factors (F1 and F3) are denoted by triangles, whereas the other factors are beyond the ranges of this plot. The ranges of the isotopic ratios for fuels supplied in Taiwan, Chinese urban particulate matter and $PM_{2.5}$ transported by EA outflows are indicated with gray squares, with relevant references noted.

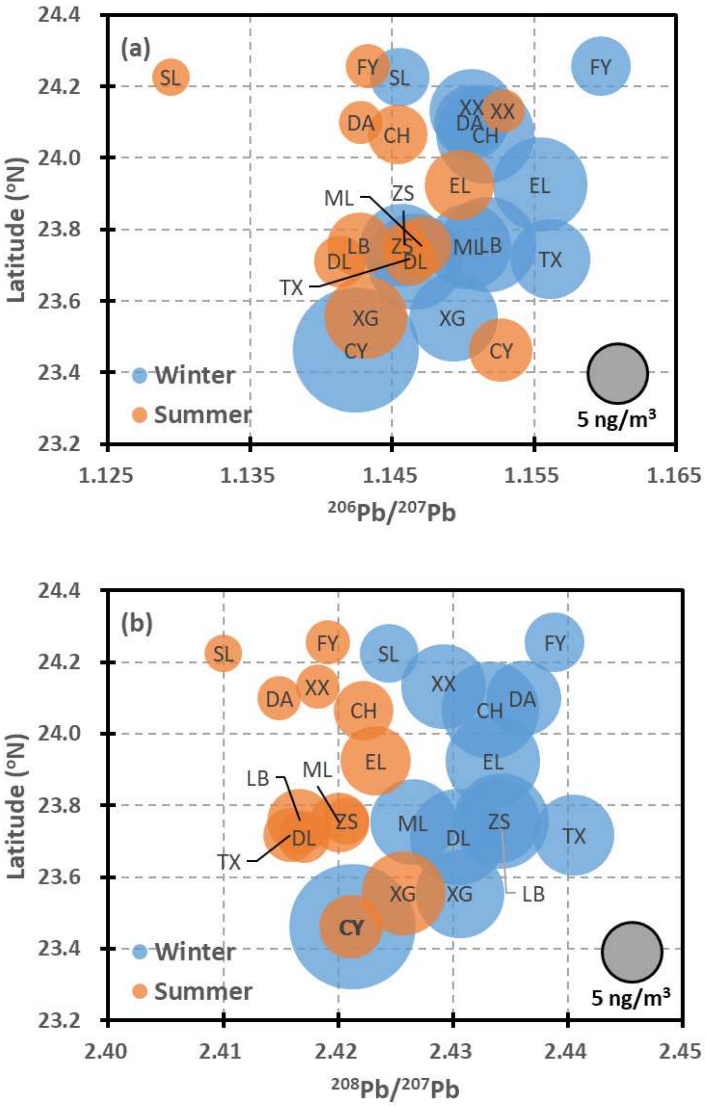

Figure 3: Geographical distribution of the ambient Pb levels and isotopic ratios, $^{206}Pb/^{207}Pb$ (a) and $^{208}Pb/^{207}Pb$ (b), along latitudes during the winter and summer campaigns. The circle area is proportional to the ambient mass concentration of Pb in $PM_{2.5}$. The labels and coordinates of the respective sampling sites are listed in Supplementary Table 1.

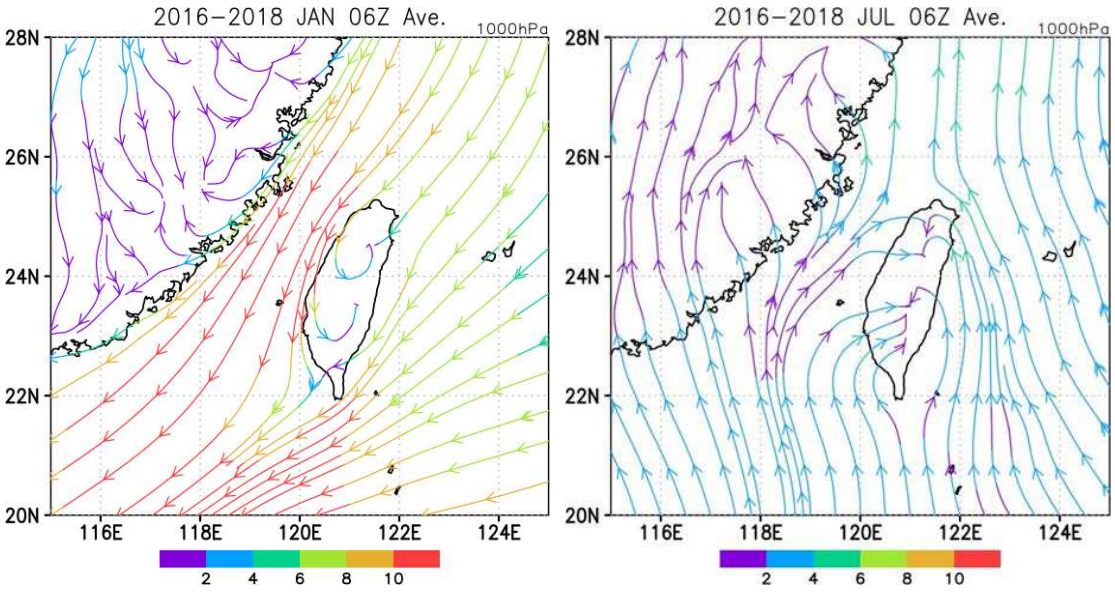

Figure 4: Mean surface streamlines in winter (January) and summer (July) from 2016–2018. The northeasterly associated East Asian winter monsoon branches reveal geographic blocking over Taiwan Island, which allows the development of side flows moving toward southeastern Taiwan. Weak southerly flows prevail during the summertime, and sea breezes dominate the transport of local air pollutants. The meteorological data at 06 UTC are used to demonstrate the general pattern of the wind field. The data are retrieved from the Global Data Assimilation System (GDAS).

Supplementary Files

This is a list of supplementary files associated with this preprint. Click to download.

- PMFPBSOURCESRSIsubmission2.pdf